Mouse hepatocytes and LSEC proteome reveal novel mechanisms of ischemia/reperfusion damage and protection by A2a receptor stimulation

Mouse hepatocytes and LSEC proteome reveal novel mechanisms of ischemia/reperfusion damage and protection by A2aR stimulation

Giorgia Mandili[1,2], Elisa Alchera[3#], Simone Merlin[3#], Chiara Imarisio[3#], BR Chandrashekar[3], Chiara Riganti[4], Alberto Bianchi[3], Francesco Novelli[1,2§], Antonia Follenzi[3§] and Rita Carini[3§].

giorgia.mandili@unito.it,alchera@med.unipmn.it,merlin@med.unipmn.it, chiara.imario@med.unipmn.it,chandrashekarbr8@gmail.com,chiara.riganti@unito.it, abianchi@med.unipmn.it,franco.novelli@unito.it,antonia.follenzi@med.unipmn.it, carini@med.unipmn.it

[1]Centre for Experimental and Clinical Studies CERMS, Azienda Universitaria Ospedaliera Città della Salute e della Scienza Città di Torino, Torino, Italy.

[2] Department of Molecular Biotechnology and Heath Sciences, University of Torino, Torino, Italy

[3]Department of Health Science, University of Piemonte Orientale , Novara, Italy

[4]Department of Oncology, University of Torino, Torino, Italy.

[#,§] These Authors equally contributed to the study

Electronic word count: 5512

Number of figures and tables: 5 figures, 3 supplementary figures, 3 supplementary tables.

Keywords: preconditioning, hepatoprotection, antioxidants, catabolic pathways, liver damage, energetic substrates.

Contact Information: Rita Carini, Department of Health Sciences, University of Piemonte Orientale 'A. Avogadro', via Solaroli, 17, Novara 28100, Italy. Telephone: 0039 0321660685; FAX: 0039 0321620421.

List of abbreviations:

HP (hepatocytes); **LSEC** (liver sinusoidal endothelial cells); **A2aR** (Adenosine 2a receptor); **IR** (Ischemia-riperfusion); **CGS21680** (2p-(2-carboxyethyl)-phenyl-amino-50-N-ethylcarboxyamido-Adenosine); **ROS** (reactive oxygen species); **2-DE** (Two-dimensional gel electrophoresis); **DIGE** (Difference gel electrophoresis).

The list of the protein abbreviations in the Supporting Information.

Financial Support: This work was supported by Fondazione Cariplo [grant number 2011-0463], ERC start up 261178 to AF. Associazione Italiana Ricerca sul Cancro 5 x mille (no. 12182) University of Turin-Progetti di Ateneo 2011 (grant Rethe-ORTO11RKTW) to FN.

Abstract

Background & Aims: Ischemia-reperfusion (IR) of liver results in hepatocytes (HP) and sinusoidal endothelial cells (LSEC) irreversible damage. Ischemic preconditioning protects IR damage upon adenosine A2a receptor (A2aR) stimulation. Understanding the phenotypic changes that underlie hepatocellular damage and protection is critical to optimize strategies against IR.

Methods: The proteome of HP and LSEC isolated from sham or IR exposed mice receiving or not the A2aR agonist CGS21680 (0.5 mg/kg b.w.) was analyzed by 2-D DIGE/MALDI-TOF.

Results: we identified 64 proteins involved in cytoprotection, regeneration, energy metabolism and response to oxidative stress; among them 34 were never reported associated to IR injury and A2aR protection. The main pathways down-regulated by IR and up- regulated by CGS21680 in HP and LSEC, were related to carbohydrate, protein and lipid supply and metabolism. In LSEC, IR reduced stress response enzymes, that were instead up-regulated by CGS21680 treatment. Functional validation experiments confirmed the metabolic involvement and showed that the inhibition of pyruvate kinase, 3-chetoacylCoA thiolase and arginase reduced the protection given by CGS21680 of *in vitro* hypoxia- reoxigenation injury, whereas their metabolic products induced liver cells protection. Moreover, LSEC, but not HP, were sensitive to H_2O_2-induced oxidative damage and CGS21680 protected against this effect.

Conclusions: IR and A2aR stimulation produces pathological and protected liver cells phenotypes respectively characterized by down- and up- regulation of proteins involved in the response to O_2 and nutrients deprivation during ischemia, oxidative stress and reactivation of aerobic energy synthesis at reperfusion. This provides novel insides in IR hepatocellular damage and protection and suggests additive therapeutic options.

Inflow occlusion during liver surgery with consequent reperfusion causes liver ischemia-reperfusion (IR) injury. IR causes up of 10% early graft dysfunction or failure during liver transplantation (1). IR injury is the result of a complex series of alterations that mainly involve hepatocytes (HP) and sinusoidal endothelial cells (LSEC) (2). Several events contribute to liver damage by IR. The lack of oxygen during the ischemic period is associated to mitochondrial de-energization, ATP depletion that impairs Ca^{2+}, H^{+} and Na^{+} homeostasis with alteration of the volume regulatory mechanisms and eventually necrosis. Upon oxygen re-admission, the uncoupled mitochondria generate reactive oxygen species (ROS) with oxidative stress, mitochondrial permeability transition and decreased capacity to synthesize ATP. These events along with caspase activation lead to cell death by both necrosis and apoptosis. Concomitantly, activation of the inflammatory reactions is also associated to the onset of IR (3,4). Minimizing the adverse effects of IR could significantly increase the number of transplantable organs and improve the outcome of the grafts (5).

Preconditioning is a powerful protective phenomenon able to activate endogenous systems that make tissues resistant to a subsequent lethal stress (6). Liver ischemic preconditioning, defined as brief periods of ischemia and reperfusion before sustained hepatic ischemia, can preserve energy loss, reduce transaminases release, inhibit inflammatory reactions and promote liver regeneration after IR injury (4,7). The surgical application of ischemic preconditioning represents a promising approach to protect against hepatic IR in humans. Its use, however, has the main disadvantage of inducing trauma to major vessels and stress to the target organ (8) and clinical studies have given conflicting results that have prevented the clinical use of ischemic preconditioning (4,8,9). These observations indicated the necessity to explore alternative approaches to activate ischemic preconditioning in patients. To this respect, pharmacological induction of liver preconditioning could represent a more efficient and reliable technique. Studies *in vitro* and *in vivo* have established a key role of the adenosine A2a receptor (A2aR) stimulation as an approach for pharmacological induction of liver preconditioning (4,10-12). Even short periods of hypoxia, in fact, lead to the enhanced breakdown of adenine nucleotides to adenosine because of the decreased production of

ATP. Accumulation of adenosine protects tissues from injury upon signalling through the adenosine receptor A2aR (4,12). Expression of new synthesized proteins can also contribute to the production of the protected liver cell phenotypes (13). The changes of protein expression of preconditioned as well as IR injured HP and LSEC are, up to now, poorly characterized. The present work analysed the proteomic patterns of primary HP and LSEC isolated from mouse liver following IR with or without pre-treatment with the A2aR agonist CGS21680 to identify new targets for the development of innovative therapeutic hepatoprotective approaches.

EXPERIMENTAL PROCEDURES

Chemicals and reagents

Protease inhibitors, nuclease, ammonium persulfate (APS), bromophenol blue, glycerol, N,N,N9,N9-tetramethylethylene-diamine (TEMED), sodium dodecyl sulfate (SDS), TRIZMA, urea, 3-[(3-cholamidopropyl) dimethylammonio]-1-propanesulphonate (CHAPS), dithiothreitol (DTT), iodoacetamide, Dulbecco's modified Eagle medium culture medium (DMEM), Trypan Blue, 2p-(2-carboxyethyl)-phenyl-amino-5-N-ethylcarboxya-mido-adenosine (CGS21680), Palmitic Acid, Non essential amino acid mixture (AA, 100X), Suramine (SUR), Norvaline (NRV), Piruvate, Trimetazidine (TMZ), 2,7-dichlorofluorescin diacetate (DCFH-DA), BCA kit, Enzymatic Assay of Pyruvate Kinase Kit and ATP Bioluminescent Assay Kit were purchased from Sigma-Aldrich (St. Louis, MO, USA). DC Protein assay kit, acrylamide, agarose, ready-made immobilized pH gradient (IPG)strip (17-cm IPG strips, pH 3-10NL) were purchased from Bio-Rad (Hercules, CA, USA). Ampholine pH 3.5–10, western blot detection system, membranes for blotting, antirabbit and antimouse IgG horseradish-peroxidase-labeled antibodies were obtained from GE Healthcare (MI, ITALY). Rabbit antibody against arginase 1 was purchased from Thermo Scientific (Illkirch Cedex, France), rabbit antibody against 3-ketoacyl-CoA thiolase from Aviva System Biology (San Diego,

CA, USA). TaqMan Gene Expression Master Mix and Taqman Gene Expression probes for mouse 3-ketoacyl-CoA thiolase, arginase 1, α-enolase and β-actin or 18S were from Applied Biosystems Italia (Monza, Italy).

Animals

Male C57BL/6 mice were used for this study purchased at Harlan srl, Italy. All animal experiments were approved by the Italian Ministry of Health and by the Università del Piemonte Orientale "A. Avogadro" Ethical Committee for Animal Care.

Ischemia-reperfusion injury

Mice were exposed for 30 min to a non lethal (-70% of the total liver volume) hepatic ischemia followed by 120 reperfusion as previously described (14). Pharmacological A2aR activation was induced by i.p. injection of CGS21680 (0.5 mg/kg of body weight) 20 min before the ischemia. Liver injury was assessed by measuring the ALT serum transaminase activity by a commercial kit (Gesan Production, ITALY) and the morphological alterations by histological observation . Details are provided in the Supporting Information.

Liver cells isolation and treatment

Liver cells were isolated by liver perfusion with collagenase digestion from sham operated mice or mice exposed to IR pretreated or not with CGS21680. HP were obtained by differential centrifugation at 50xg for 5 min at 4°C and LSEC by immunomagnetic separation using a negative selection with a mouse anti-CD45 and positive selection with anti-CD146 antibodies linked to immunomagnetic beads (Miltenyibiotec, Calderana di Reno, BO, ITALY) as previously reported (15) and described in details in the Supporting Information.

Isolated HP and LSEC for proteomic analysis were stored at -80°C until solubilization.

For evaluation of hypoxia-reoxygenation injury, primary HP and LSEC were resuspended (10^6/mL cell density) in Viaspan solution (University of Wisconsin solution without additives) and fluxed with 95% N2/5% CO2 and maintained at 4°C for 16 hours in sealed flasks. For reoxygenation, cells were transferred to an oxygenated Krebs-Henseleit buffer containing 20 nmol/L N-(2-

hydroxyethyl)-piperazine-N0-(2-ethanesulfonic acid) (pH 7.4 at 37°C), and the incubation flasks were further fluxed with a 95% air/5% CO_2 gas mixture. When indicated, liver cells, suspended in the Viaspan solution, were pre-incubated 15 min at 37° C before cold preservation with CGS21680 (5 μmol/l) and/or suramine (SUR, 20 μmol/l), norvaline (NRV, 50 μmol/l), trimetazidine (TMZ, 100 μmol/l), pyruvate (10 μmol/l), palmitic acid (PA, 2 μmol/l) or non-essential amino acid mixture (AA, 10%). To evaluate oxidative damage, HP or LSEC in Krebs-Henseleit buffer, were treated with H_2O_2 (500 μmol/l) in presence or in absence of CGS21680 (5 μmol/l) and incubated for 30 min at 37°C under a 95% air/5% CO_2 gas atmosphere.

Determination of Cell Viability

Cell viability was estimated by the determination of nuclear fluorescence staining with propidium iodide using a FACScan analyzer (Becton-Dickinson, San Jose, CA) and CellQuest software (Becton-Dickinson) (13).

Measurement of Reactive Oxygen Species (ROS)

Intracellular ROS production was measured as reported in (14) by measuring the DCFH-DA (2,7-dichlorofluorescin diacetate) fluorescence intensity with a Hitachi F-4500 fluorescence spectrophotometer. Details are provided in the Supporting Information.

Data Analysis

Statistical analysis was performed with InStat 3 statistical software (GraphPad Software, Inc., San Diego, CA) by 1-way analysis of variance testing with Bonferroni correction for multiple comparisons when more than 2 groups were analyzed. The distribution normality of all groups was preliminarily verified with the Kolmogorov and Smirnov test. Significance was established at the 5% level.

Proteomic analysis

Two-dimensional gel electrophoresis (2-DE) on ready-made IPG strip (17-cm IPG strips, pH 3-10NL) were performed essentially as described (16). For 2-D DIGE analysis fifty micrograms of each sample (control, CGS21680, IR or CGS21680+IR) were minimally labelled with CyDye

DIGE Fluors following the manufacturer's instruction (GE Healthcare). For 2DE coomassie stained gel, 1 mg of total liver protein was loaded. Destaining and in-gel enzymatic digestion of G-stained spots were performed as previously described (16). All digests were analyzed by MALDI-TOF (TofSpec SE, MicroMass). Details are provided in the Supporting Information.

To verify the significance of the proteins expression variations two-sided Student's t test was used. Experiments were performed in triplicate. Statistical significance was set at p values$\leq$0.05. Proteins were classified as differentially expressed if ratio in spot intensity was greater than 1.5-fold (protein over-expressed) or lower than 0.5-fold (protein under-expressed).

The protein and RNA levels of ketoacyl-CoA thiolase, arginase 1 and α-enolase were evaluated by western blotting and RT-PCR analysis as described in the Supporting Information.

Enzymatic assays

Aldolase B activity was measured as described in (17), with minor modifications. α-enolase activity was measured accordingly to (18). The activity of pyruvate kinase was detected with the Enzymatic Assay of Pyruvate Kinase kit, following the manufacturer's instruction. Fatty acids β-oxidation was measured as previously reported (19), with minor modifications. The activity of carbamoyl phosphate synthetase I was measured on mitochondrial extracts, isolated as previously reported (20). Arginase activity was measured by a spectrophotometric method (21). To measure the isocitrate dehydrogenase activity, 25 µg mitochondrial proteins were re-suspended in 0.3 mL of Tris-acetate (pH 7.4), containing 5 mmol/L DL-isocitrate trisodium salt and 5 mmol/L $MgCl_2$. The reaction was started by adding 0.5 mmol/L NAD^+ and the absorbance at 340 nm was followed for 5 minutes. Results were expressed as nmol NADH/mg mitochondrial proteins. The rate of cytochrome c reduction was measured according to (22) with minor modifications. The ATP level in mitochondria extracts was measured with the ATP Bioluminescent Assay Kit. Additional details are provided in the Supporting Information.

RESULTS

Analysis of liver injury following IR and A2aR stimulation

Mice exposure to 30 min of hepatic ischemia followed by 120 min reperfusion caused substantial liver injury as determined by the serum ALT (alanine transaminase) release and hepatic histology (Supplementary Fig. 1). In accordance to previous observations (4,12), stimulation of adenosine A2 receptors by mice treatment with CGS21680 (0.5 mg/kg b.w.) before IR significantly reduced the serum ALT increase and markedly attenuated the signs of hepatocyte necrosis and sinusoidal congestion detected by hematoxylin and eosin staining (Supplementary Fig. 1).

Proteomic analysis following IR and A2aR stimulation

2-D DIGE proteomic analysis was performed to elucidate the phenotypic changes of HP and LSEC isolated from mice livers exposed to IR with or without A2aR stimulation (Supplementary Fig.2, Supplementary Tables 1,2,3)

By comparing HP and LSEC of sham operated mice *vs* mice subjected to IR, we observed that 16 proteins were down-regulated (Fig. 1, Supplementary Table 1). In particular, in both HP and LSEC, IR reduced proteins involved in glycid, lipid and mitochondrial (Krebs cycle and oxidative phosphorylation) metabolism. Notably, IR decreased, in LSEC specifically, two proteins related to the response to oxidative stress (Fig.1).

Compared to control, treatment with the A2aR agonist CGS 21680 alone affected the expression of metabolic proteins: 6 were up-regulated and 1 was down-regulated (Fig. 1, Supplementary Table 2).

The treatment with CGS21680 and IR *vs* control, with the exception of three proteins that were down-regulated in HP, up-regulated 10 proteins, mostly metabolic enzymes associated to ATP synthesis, glycolysis, lipid and aminoacid catabolism, and cell response to stress (Fig. 1, Supplementary Table 3). Notably the CGS treatment completely rescued the expression of the 16

proteins down-regulated by IR, with 14 proteins that recovered control level and two that were up-regulated (Fig. 1, Supplementary Table 3).

It is noteworthy, that when cell extracts obtained from mice receiving CGS21680 with IR were compared to those exposed to IR alone evidenced a more complex and unexpected scenario. We found, that further 19 proteins, including metabolic, stress-related and folding-related proteins, were up-regulated (Fig. 1, Supplementary Table 3).

Also the comparison IR plus CGS21680 *vs* CGS21680 did not reproduce the protein profile of IR alone (Fig. 1, Supplementary Table 1 and 3). We detected the modulation of 41 proteins and, most intriguingly, 34 of them were up-regulated whereas in IR vs control all proteins were down-regulated. Among the up-regulated proteins, we evidenced metabolic and stress related enzymes.

Altogether, in both HP and LSEC, A2aR stimulation by CGS21680 alone and, even more when followed by IR, up-regulated proteins associated to DNA synthesis and cytoprotection. Intriguingly, the pathways mainly involved were related to cell response to stress and, more markedly, to the carbohydrate, lipid, and amino acids supply and catabolism (Fig. 2). Thus suggesting a possible role of the antioxidant and of the catabolic enzymes in the hepatoprotective effects of A2aR stimulation.

Proteomic data have been validated by western blot and RT-PCR analysis on three key metabolic enzymes (ENOA, THIM and ARGI1) (Supplementary Fig. 3).

Functional validation of the metabolic effect of A2aR stimulation on HP and LSEC

Proteomic data showed that A2aR stimulation increased the expression of several catabolic enzymes, that were instead reduced following IR (Fig.1, Supplementary Table 1,2 and 3). To functionally confirm this observation, the activity of several enzymes referred to glycid, lipid, aminoacid and mitochondrial metabolism was assayed.

The activity of glicolytic enzymes α-enolase (ENOA) and pyruvate kinase (KPYR) was down-regulated by IR and up-regulated by IR plus CGS21680 in HP and LSEC, whereas that of fructose-

bisphosphate aldolase B (ALDOB) was down-regulated by IR and up-regulated by IR plus CGS21680 in HP only (Fig. 3).

For lipid metabolism, we evaluated the products of β-oxidation reactions, that were down-regulated by IR and up regulated by IR plus CGS21680 in HP and LSEC (Fig. 3).

For aminoacid catabolism, the activity of two enzymes linked to urea cycle, namely carbamoyl-phosphate synthase (CPSM) and arginase 1 (ARGI1) was evaluated. The activity of CPSM was reduced by IR (although not significantly in LSEC) and strongly up-regulated by IR plus CGS21680 (Fig. 3). The activity of ARGI1 was significantly down regulated by IR and up-regulated by IR plus CGS21680 in HP only.

For mitochondrial metabolism, the activity of isocitrate dehydrogenase (IDHC) and cytochrome C, and the ATP production were measured. The activity of IDHC and cytochrome C was significantly down-regulated by IR and up-regulated by IR plus CGS21680 in both HP and LSEC, whereas ATP production was the same but only in HP (Fig. 3).

These data clearly indicate that IR strongly reduces the metabolism and that CGS21680 rescues it in both HP and LSEC, confirming the observations obtained by proteomic approach.

Functional validation of the cytoprotective role of metabolic enzymes in A2aR-induced resistance to death of HP and LSEC

To evaluate the cytoprotective meaning of the up-regulation of the metabolic enzymes in HP and LSEC obtained from mice treated with CGS21680 before hepatic IR, we applied an *in vitro* model of IR injury using primary HP and LSEC preserved in hypoxic conditions in VIASPAN solution and then re-oxygenated in Krebs-Henseleit at 37° C. As shown in Figure 4A, chemical inhibition of the 3 key enzymes of carbohydrate, lipid and aminoacids catabolism, pyruvate kinase (KPYR), 3-ketoacyl-CoA thiolase (THIM) and arginase 1 (ARGI1) by suramine (SUR, 20 μmol/L), trimetazidine (TMZ, 100 μmol/L) and norvaline (NRV, 50 μmol/L) respectively, significantly reduced the protection given by CGS21680 against reperfusion damage. On the same line, supplementing VIASPAN solution with palmitic acid (2 μmol/L), a non-essential aminoacid

mixture (10%) or pyruvate (10 μmol/L) significantly reduced HP and LSEC mortality induced by 60 min reoxygenation, partially reproducing the cytoprotective action of CGS21680 (5μmol/L) supplementation (Fig.4B).

Functional validation of the antioxidant effect of A2aR stimulation on LSEC

Proteomic data showed that A2aR stimulation increased the expression of several antioxidant enzymes, that were instead reduced following IR, particularly in LSEC (Fig.1, Supplementary Table 1,2 and 3). These observations were functionally confirmed by evaluating the susceptibility to oxidative stress of primary mouse HP and LSEC upon 30 min exposure to H_2O_2 (500 μmol/L). H_2O_2 treatment significantly increased ROS and cell damage in LSEC but not in HP. The stimulation of A2aR with CGS21680 abolished ROS production and prevented the loss of LSEC viability induced by H_2O_2 exposure (Fig.5).

DISCUSSION

Ischemia/reperfusion damage causes up to 10% of early organ graft failure following liver transplantation, and can lead to a higher incidence of both acute and chronic rejections. Minimizing the adverse effects of this injury could significantly increase the number of transplantable livers improving the outcome of the grafts (5-7). Ischemic preconditioning demonstrated its efficacy in several models (2-7) and different pharmacological preconditioning approaches have been developed to overcome limitations of surgical preconditioning (2-7,13). Previous studies have shown that pre-treatment with the A2aR agonist CGS21680 enhanced tolerance against hepatic IR damage (4,11). This work describes for the first time the proteome alterations of mouse HP and LSEC isolated from livers exposed to IR in the presence or absence of A2aR stimulation elucidating the liver cells contribution to IR damage and hepatoprotection by pharmacological preconditioning.

Our work has pointed out profound modifications of HP and LSEC proteome and enzymatic activities contributing to clarify critical processes involved in IR injury and liver preconditioning, implementing and dissecting the previous observations obtained in entire liver (24-29).

Considering all identified proteins, few of the affected proteins were shared between HP and LSEC, highlighting the diversity of these cells and the importance to analyse them separately. However the pathways involved were almost the same (metabolism, stress response, protein folding and regeneration), showing a general common response, but with the prevalence of metabolic effects in HP and stress-related effects in LSEC. Notably, the profiling of the enzymatic and functional activities reduced by IR and rescued by CGS21680 were almost completely overlapped with those observed by proteomics.

The severe ATP depletion during ischemic phase in HP has been generally ascribed to the lack of O_2 and glycolytic substrates supply consequent to blood interruption (2-4). Such alteration is however prevented in preconditioned ischemic liver, indicating that the block of blood supply is not *per se* sufficient to justify the ATP loss. In addition, one of the most striking alteration of IR injured liver is its incapability of recovering aerobic ATP production at blood flow reestablishment with reperfusion. The observation that glycolytic enzymes and ATP synthases subunits were decreased in HP and LSEC derived from liver exposed to IR and that CGS21680 treatment combined to IR up-regulated the glycolytic and mitochondrial pathways endorses the hypothesis that IR damage is not merely due to a reduction of blood flow requirement, but to a coordinate perturbation of metabolic enzymes expression, that is rescued by preconditioning.

Furthermore, the liver acts as a major organ for lipid metabolism and that hepatic aerobic ATP synthesis is strictly dependent on lipid supply and catabolism. Interestingly we found that CGS21680 treatment is able to promote the lipid transport and β-oxidations, which were instead down-modulated by IR. It would be interesting in the future to evaluate the impact of β-oxidation modulation to prevent IR injury.

The up-regulation of urea cycle enzymes and the increase of activity of two key enzymes of this pathway (CPSM and ARGI1) following CGS21680 treatment was observed. This suggests that the improvement of amino acids catabolism could represent a response of HP and LSEC to ATP deprivation caused by IR.

All together, these results indicated that the down-regulation of key metabolic enzymes can explain the ATP loss caused by IR. Therefore, A2aR stimulation provides a general metabolic advantage to HP and LSEC, demonstrated by ATP production increasing, not only rescuing the metabolic alteration induced by IR but in some cases enhancing the expression of enzymes required for energy production.

The relevance of our observations about the metabolic advantage provided by CGS21680 is also supported by the fact that the cytoprotective action of CGS21680 is reverted by the inhibition of pyruvate kinase (KPYR), 3-ketoacyl-CoA thiolase (THIM) and arginase (ARGI1), three enzyme of glycolysis, β-oxidation and urea cycle respectively, that are impaired by IR. Furthermore, cell supplementation with the glycolic end-product pyruvate, the free fatty acid palmitic acid or aminoacid mixture demonstrated to partly mimic the protective effects of CGS21680 against HP and LSEC hypoxia-reoxygenation damage.

Notably among the 28 metabolic proteins identified, only 14 of them were already connected to IR and preconditioning (FABPL, ATPB, FABPI, ENOA, ATPA, ARGI1, ALDOB, ETFA, THIM, CPSM, TPIS, OTC, HINT, FABP5) (5, 25-27, 29-32), while the others are completely new (GLYC, IDHC, KPYR, DHSO, FAAA, S2542, PGK1, CLC4F, ODBA, NDKB, ATP5H, PROSC, ECH1, AL4A1).

Another fundamental aspect is the role of antioxidant enzymes in the protection against IR injury by preconditioning. We detected several proteins involved in liver cell response to oxidative stress. Many of these proteins (GRP75, GSTP1, SBP2, PPIA, GSTM1, CATA, PRDX6, CH60, PDIA3) were already known to be involved in IR and preconditioning processes (5, 25-29). Catalase, GSTP1, GSTP2 and GSTM1 are directly linked to detoxification of ROS and GSH is known as

highly effective antioxidant present in elevated concentrations in HP (34). PRDX6 is another well-known antioxidant demonstrated to normalize mitochondrial respiration during IR (27). Finally, the chaperones GRP75, PDIA1, PDIA3, CH60 can be involved in protein folding repair mechanism, together with the 2 proline isomerase PPIA and FKB1B, since ROS are known to cause protein misfolding (35). The majority of stress proteins that we have identified have mitochondrial origin, confirming previous observation (29, 36).

We observed that CGS21680 treatment generally increased the antioxidant defences particularly in LSEC, whereas IR depressed the antioxidant enzymes content in LSEC exclusively and that CGS21680 treatment of these cells prevented oxidative damage following in vitro addition of H_2O_2. These results may explain the high sensitivity of LSEC to cold ischemia and the microcirculatory disturbance induced by IR damage as well as the rescuing action of ischemic preconditioning (2).

An intriguing aspect that may deserve further analysis is that the combined treatment of CGS21680 plus IR results often more effective in producing protective protein modifications than that with CGS21680 alone. This suggests that the genomic changes induced by A2aR stimulation accomplish a full-protected phenotype only in presence of cell stress. Indeed recent results showed that A2aR stimulation might effectively prevent also pathological conditions different by IR through the activation of noxious-specific mechanisms of protection (37).

In conclusion, this study contributed to the understanding of the molecular bases of IR injury and cytoprotection by A2aR stimulation, showing specific modifications of HP and LSEC proteomes. The great number of new proteins identified demonstrate the strength of our experimental approach. Finally this study, showing the importance of glycid, lipid, aminoacids and antioxidants availability in IR injury and in A2aR-induced liver cell protection, suggest the protective potential of supplementing organ preservation solutions with energy-linked metabolites and natural or synthetic antioxidants.

REFERENCES

1. Fondevila C, Busuttil RW, Kupiec-Weglinski JW. Hepatic ischemia/reperfusion injury—a fresh look. Exp Mol Pathol 2003; 74:86-93.

2. Peralta C, Jiménez-Castro MB, Gracia-Sancho J. Hepatic ischemia and reperfusion injury: effects on the liver sinusoidal milieu. J Hepatol 2013; 59:1094-106.

3. Jaeschke H. Molecular mechanisms of hepatic ischemia-reperfusion injury and preconditioning. Am J Physiol Gastrointest Liver Physiol 2003; 284:G15-26.

4. Alchera E, Dal Ponte C, Imarisio C, Albano E, Carini R. Molecular mechanisms of liver preconditioning. World J Gastroenterol 2010; 16:6058-6067.

5. Vascotto C, Cesaratto L, D'Ambrosio C, Scaloni A, Avellini C, Paron I, Baccarani U et al. Proteomic analysis of liver tissues subjected to early ischemia/reperfusion injury during human orthotopic liver transplantation. Proteomics 2006; 6:3455-3465.

6. Yellon DM, Dana A. The preconditioning phenomenon: A tool for the scientist or a clinical reality? Circ Res 2000; 87:543-50.

7. De Rougemont O, Lehmann K, Clavien PA. Preconditioning, Organ Preservation, and Postconditioning to Prevent Ischemia-Reperfusion Injury to the Liver. Liver Transpl 2009; 15:1172–1182.

8. Franchello A, Gilbo N, David E, Ricchiuti A, Romagnoli R, Cerutti E, Salizzoni M. Ischemic preconditioning (IP) of the liver as a safe and protective technique against ischemia/reperfusion injury (IRI). Am J Transplant 2009; 9:1629-1639.

9. Scatton O, Zalinski S, Jegou D, Compagnon P, Lesurtel M, Belghiti J, Boudjema K, et al. Randomized clinical trial of ischaemic preconditioning in major liver resection with intermittent Pringle manoeuvre. Br J Surg 2011; 98:1236-1243.

10. Peralta C, Hotter G, Closa D, Gelpí E, Bulbena O, Roselló-Catafau J. Protective effect of preconditioning on the injury associated to hepatic ischemia-reperfusion in the rat: role of nitric oxide and adenosine. Hepatology 1997; 25:934–937.

11. Ben-Ari Z, Pappo O, Sulkes J, Cheporko Y, Vidne BA, Hochhauser E. Effect of adenosine A2A receptor agonist (CGS21680) on ischemia/reperfusion injury in isolated rat liver. Apoptosis 2005; 10:955-62.

12. Caldwell CC, Tschoep J, Lentsch AB. Lymphocyte function during hepatic ischemia/reperfusion injury. J Leukoc Biol 2007; 82:457-464.

13. Alchera E, Tacchini L, Imarisio C, Dal Ponte C, De Ponti C, Gammella E, Cairo G, et al. Adenosine-dependent activation of hypoxia-inducible factor-1 induces late preconditioning in liver cells. Hepatology 2008; 48:230-9.

14. Dal Ponte C, Alchera E, Follenzi A, Imarisio C, Prat M, Albano E, Carini R. Pharmacological postconditioning protects against hepatic ischemia/reperfusion injury. Liver Transpl 2011; 17:474-82

15. Follenzi A, Benten D, Novikoff P, Faulkner L, Raut S, Gupta S. Transplanted endothelial cells repopulate the liver endothelium and correct the phenotype of hemophilia A mice. J Clin Invest 2008; 118:935-45.

16. Mandili G, Marini C, Carta F, Zanini C, Prato M, Khadjavi A, Turrini F, Giribaldi G. Identification of phosphoproteins as possible differentiation markers in all-trans-retinoic acid-treated neuroblastoma cells. PLoS One 2011; 6:e18254.

17. Dawson NJ, Biggar KK, Storey KB. Characterization of fructose-1,6-bisphosphate aldolase during anoxia in the tolerant turtle, Trachemys scripta elegans: an assessment of enzyme activity, expression and structure. PLoS One 2013; 8:e68830

18. Beutler, E. Red cell metabolism. A manual of biochemical methods. New York and London: Grune & Stratton; 1975

19. Gaster M, Rustan AC, Aas V, Beck-Nielsen H. Reduced Lipid Oxidation in Skeletal Muscle From Type 2 Diabetic Subjects May Be of Genetic Origin. Evidence From Cultured Myotubes. Diabetes 2004; 53:542-548

20. Campia I, Lussiana C, Pescarmona G, Ghigo D, Bosia A, Riganti C. Geranylgeraniol prevents the cytotoxic effects of mevastatin in THP-1 cells, without decreasing the beneficial effects on cholesterol synthesis. Br J Pharmacol 2009; 158:1777-1786

21. Giri H, Chandel S, Dwarakanath LS, Sreekumar S, Dixit M. Increased endothelial inflammation, sTie-2 and arginase activity in umbilical cords obtained from gestational diabetic mothers. PLoS One 2013; 8:e84546

22. Wibom R, Hagenfeldt L, von Dobeln U. Measurement of ATP production and respiratory chain enzyme activities in mitochondria isolated from small muscle biopsy samples. Anal Biochem 2002; 311: 139–151

23. Song X, Zhang N, Xu H, Cao L, Zhang H. Combined preconditioning and postconditioning provides synergistic protection against liver ischemic reperfusion injury. Int J Biol Sci 2012; 8:707-18.

24. Vascotto C, Cesaratto L, D'Ambrosio C, Scaloni A, Avellini C, Paron I, Baccarani U et al. Proteomic analysis of liver tissues subjected to early ischemia/reperfusion injury during human orthotopic liver transplantation. Proteomics 2006; 6:3455-65.

25. Wilson CH, Zeile S, Chataway T, Nieuwenhuijs VB, Padbury RT, Barritt GJ. Increased expression of peroxiredoxin 1 and identification of a novel lipid-metabolizing enzyme in the early phase of liver ischemia reperfusion injury. Proteomics 2011; 11:4385-96.

26. Xu C, Zhang X, Yu C, Lu G, Chen S, Xu L, Ding W et al. Proteomic analysis of hepatic ischemia/reperfusion injury and ischemic preconditioning in mice revealed the protective role of ATP5beta. Proteomics 2009; 9:409-19.

27. Eismann T, Huber N, Shin T, Kuboki S, Galloway E, Wyder M, Edwards MJ et al. Peroxiredoxin-6 protects against mitochondrial dysfunction and liver injury during ischemia-reperfusion in mice. Am J Physiol Gastrointest Liver Physiol 2009; 296:G266-74.

28. Raza A, Dikdan G, Desai KK, Shareef A, Fernandes H, Aris V, de la Torre AN, et al. Global gene expression profiles of ischemic preconditioning in deceased donor liver transplantation. Liver Transpl 2010; 16:588-99.

29. Moon KH, Hood BL, Mukhopadhyay P, Rajesh M, Abdelmegeed MA, Kwon YI, Conrads TP,et al. Oxidative inactivation of key mitochondrial proteins leads to dysfunction and injury in hepatic ischemia reperfusion. Gastroenterology 2008; 135:1344-57.

30. Martin J, Romanque P, Maurhofer O, Schmitter K, Hora C, Ferrand G, Dufour JF. Ablation of the tumor suppressor histidine triad nucleotide binding protein 1 is protective against hepatic ischemia/reperfusion injury. Hepatology 2011; 53:243-52.

31. Jeyabalan G, Klune JR, Nakao A, Martik N, Wu G, Tsung A, Geller DA. Arginase blockade protects against hepatic damage in warm ischemia-reperfusion. Nitric Oxide 2008; 19:29-35.

32. Wang X, Pan L, Lu J, Li N, Li J. N-3 PUFAs attenuate ischemia/reperfusion induced intestinal barrier injury by activating I-FABP-PPARγ pathway. Clin Nutr 2012; 31:951-7.

33. Wouters BG, Koritzinsky M. Hypoxia signalling through mTOR and the unfolded protein response in cancer. Nat Rev Cancer 2008; 8:851-64.

34. Jaeschke H, Woolbright BL. Current strategies to minimize hepatic ischemia-reperfusion injury by targeting reactive oxygen species. Transplant Rev (Orlando) 2012; 26:103-14.

35. Gregersen N, Bross P. Protein misfolding and cellular stress: an overview. Methods Mol Biol 2010; 648:3-23.

36. Varela AT, Simões AM, Teodoro JS, Duarte FV, Gomes AP, Palmeira CM, Rolo AP. Indirubin-3'-oxime prevents hepatic I/R damage by inhibiting GSK-3beta and mitochondrial permeability transition. Mitochondrion 2010; 10:456-63.

37. Imarisio C, Alchera E, Sutti S, Valente G, Boccafoschi F, Albano E, Carini R. Adenosine A(2a) receptor stimulation prevents hepatocyte lipotoxicity and non-alcoholic steatohepatitis (NASH) in rats. Clin Sci (Lond) 2012; 123:323-32.

FIGURE LEGENDS

Figure 1

Differentially expressed proteins upon IR, A2aR stimulation or A2aR stimulation plus IR.

Down-regulated (black) and up-regulated (white) identified proteins associated or not (others) to metabolism (glycid, lipid, mitochondrial and aminoacid metabolism) or stress-response/folding processes in control conditions or upon A2aR stimulation with the A2aR agonist CGS21680 or IR in presence or in absence of CGS21680 treatments. All pair conditions were examined.

Figure 2

Graphical abstract of the main pathways involved in IR and A2aR stimulation in HP and LSEC. Identified proteins are indicated.

Figure 3

Effects of IR, A2aR stimulation or A2aR stimulation plus IR on metabolic activities.

Enzymatic activities of (A) fructose-bisphosphate aldolase B (ALDOB), α-enolase (ENOA), and pyruvate kinase (KPYR), of (B) β-oxidation reactions, of (C) carbamoyl-phosphate synthase (CPSM) and arginase 1 (ARGI1) and of (D) isocitrate dehydrogenase (IDHC), cytochrome C and the ATP production were evaluated in HP and LSEC. The results are means ± S.D. of four experiments. *$p<0,01$, #$p\leq0,05$

Figure 4

A2aR stimulation protects HP and LSEC against hypoxia-reoxygenation injury by promoting glycid, lipid and aminoacids catabolism.

Viability of primary mice HP and LSEC conserved for 16 hours in cold hypoxic conditions and exposed to 60 minutes of warm reoxygenation.

HP and LSEC were conserved in VIASPAN solution in presence or in absence of: A) the 3-ketoacyl-CoA thiolase inhibitor trimetazidine (TMZ, 100 μmol/L), the arginase inhibitor norvaline (NRV, 50 μmol/L) and the pyruvate kinase inhibitor suramine (SUR, 20 μmol/L), with or without

the A2aR agonist CGS21680 (5 μmol/L) or B) palmitic acid (2 μmol/L) (PA), non essential aminoacids mixture (10%) (AA), pyruvate (10 μmol/L) or CGS21680 (5 μmol/L).

The results are means ± S.D. of four experiments. *p<0,001, #p<0,01

Figure 5

CGS21680 prevents oxidative species production and oxidative damage of LSEC.

Intracellular oxidative species production evaluated as DCFH-DA intracellular fluorescence intensity (A) and viability (B) of primary mice HP and LSEC after 30 min exposure to H_2O_2 (500 μmol/L). The results are means ± S.D. of four experiments. *p<0,001, #p<0,01.

Acknoledgements

We thank prof. E. Albano for critically revising the manuscript.

Figure

Click here to download high resolution image

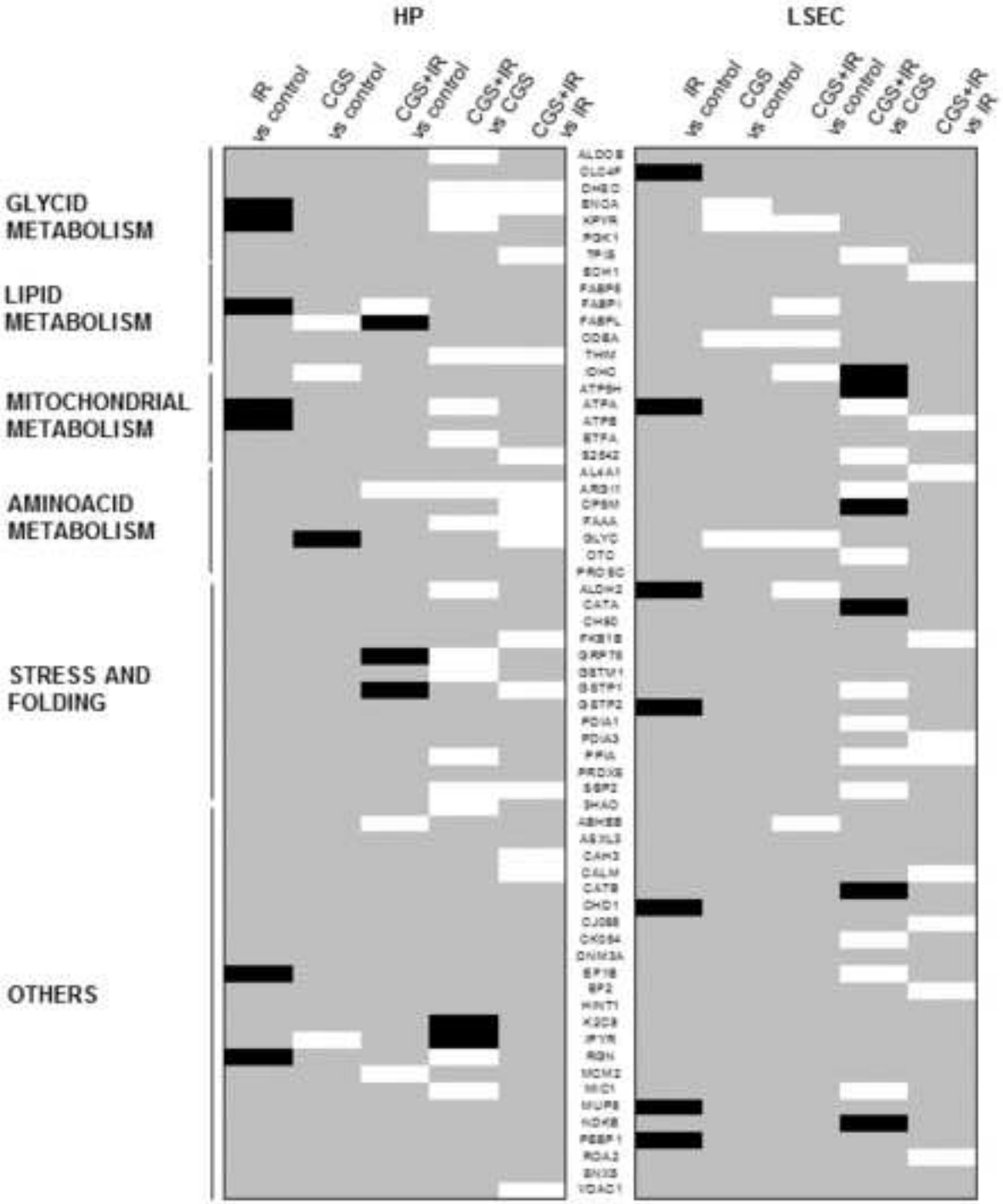

Figure 1

Figure

Click here to download high resolution image

Figure 2

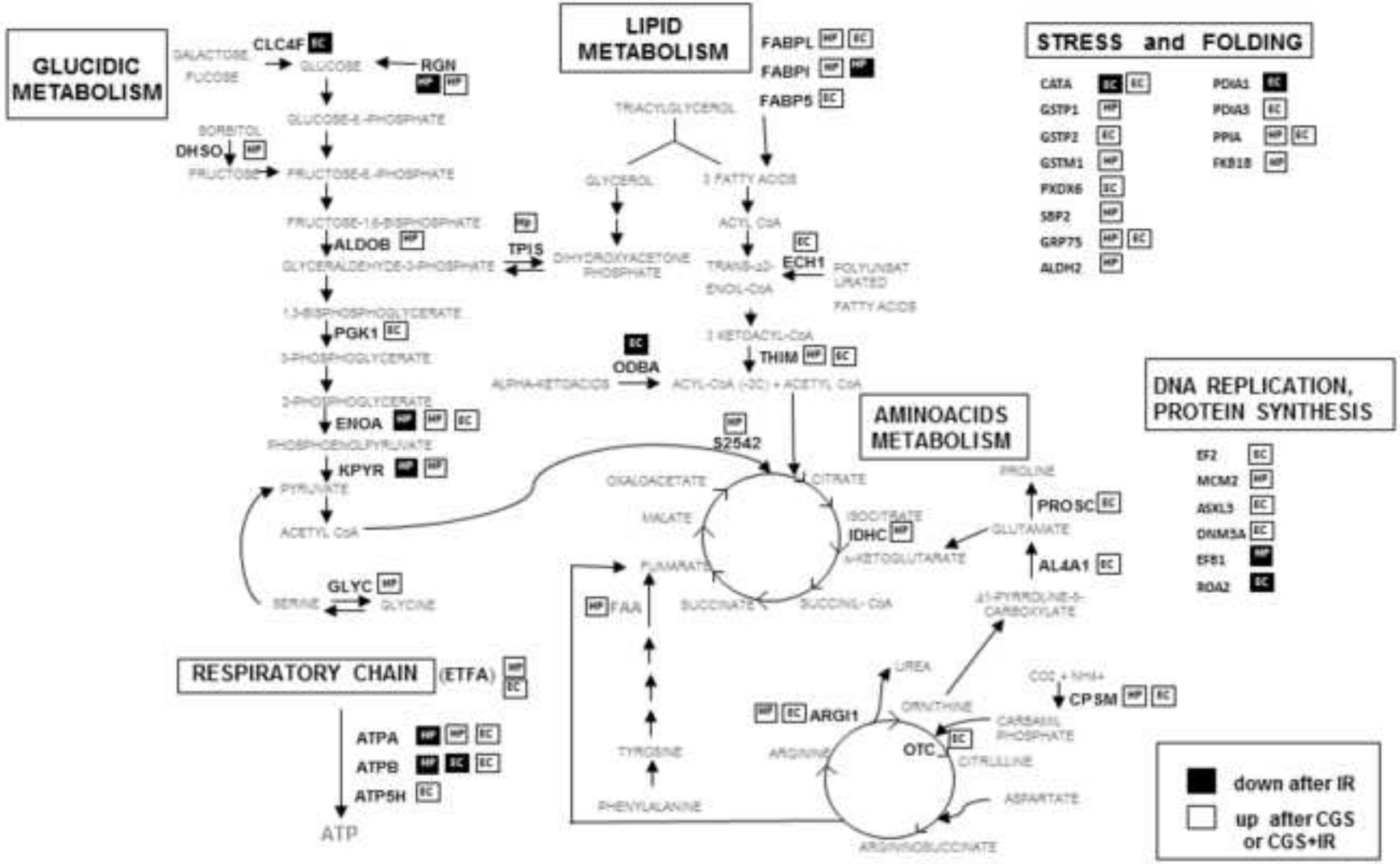

Figure

Click here to download high resolution image

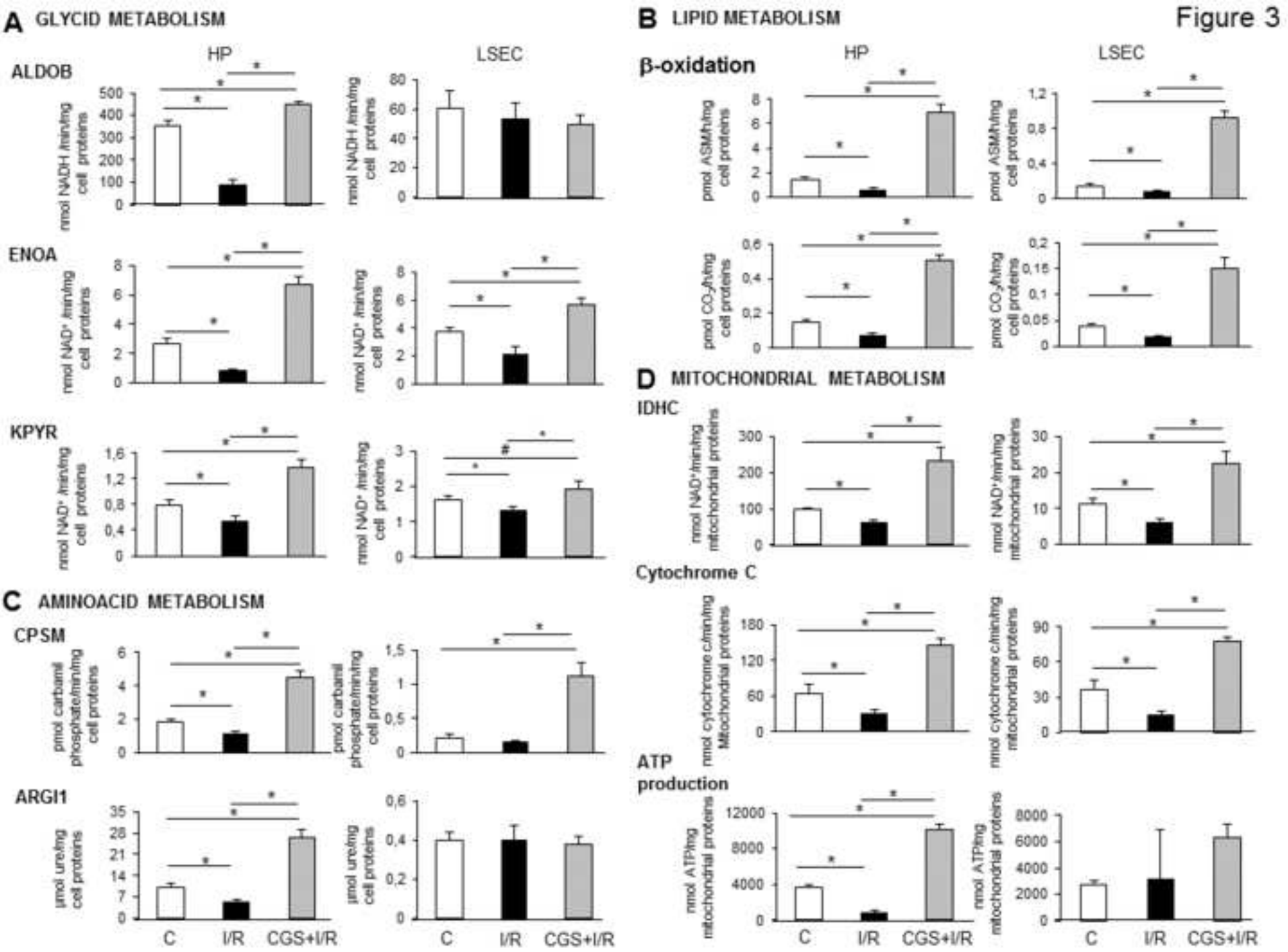

Figure 3

Figure

Click here to download high resolution image

Figure 4

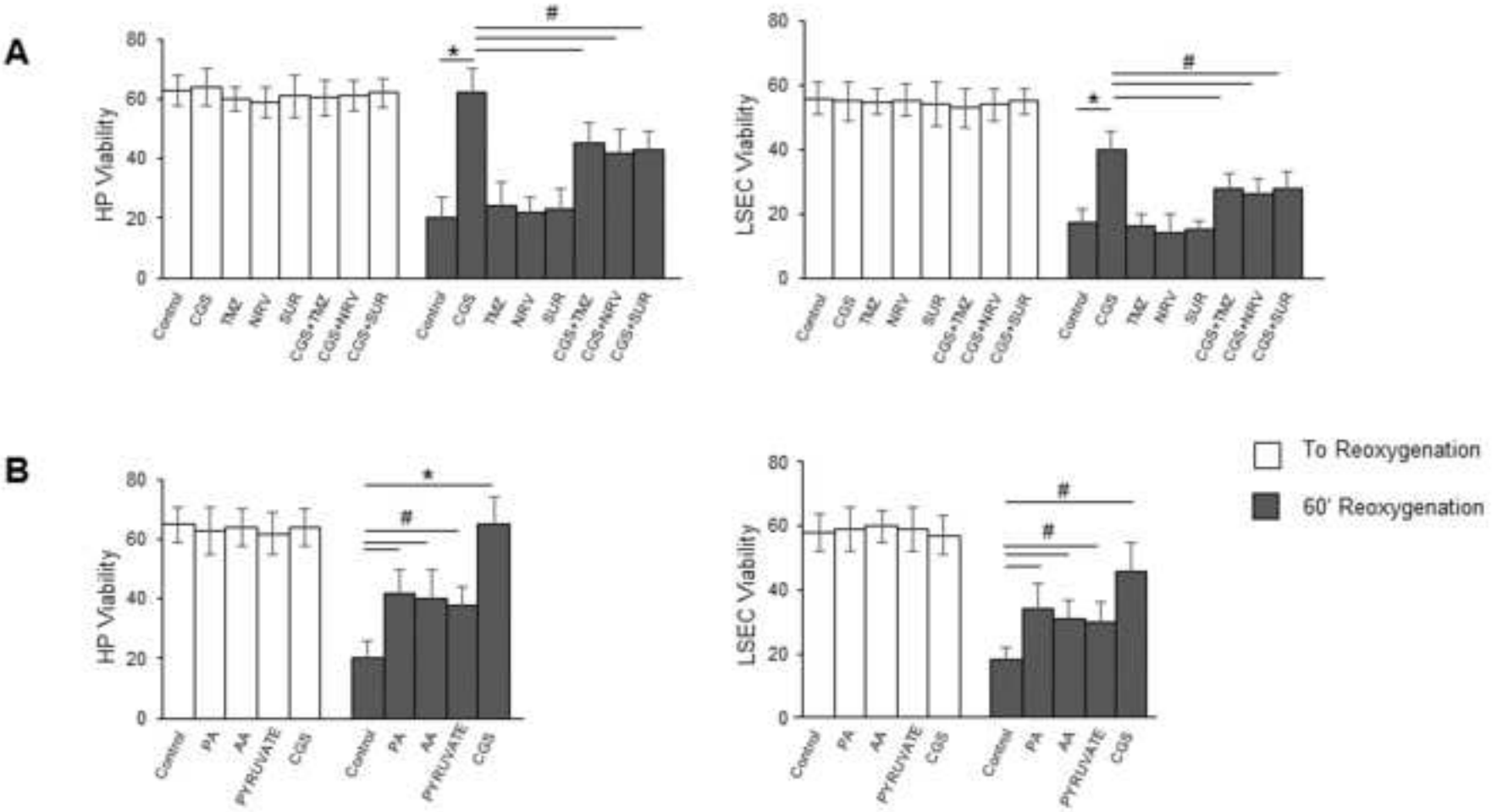

Figure

Click here to download high resolution image

Figure 5

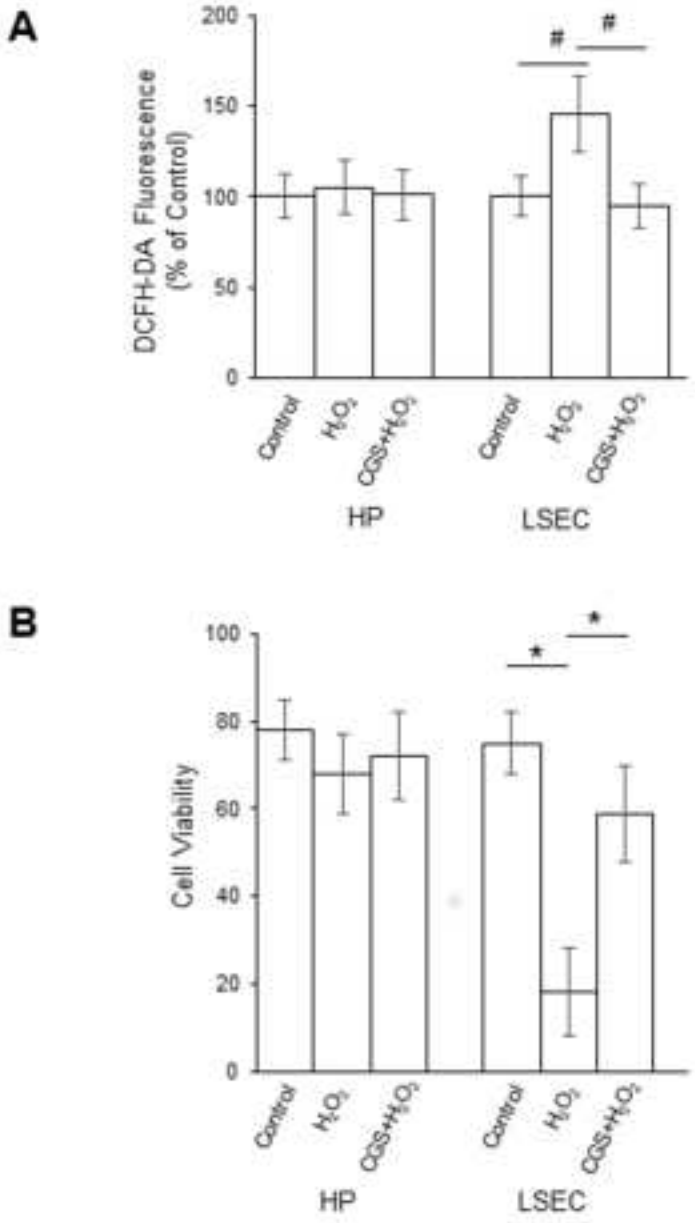

SUPPLEMENTARY MATERIAL

Mouse hepatocytes and LSEC proteome reveal novel mechanisms of ischemia/reperfusion damage and protection by A2a receptor stimulation.

Giorgia Mandili, Elisa Alchera, Simone Merlin, Chiara Imarisio, BR Chandrashekar, Chiara Riganti, Alberto Bianchi, Franco Novelli, Antonia Follenzi and Rita Carini.

Table of content:

SUPPORTING INFORMATION

EXPERIMENTAL PROCEDURES

Ischemia-reperfusion injury

Male C57BL6 mice were anesthetized with isoflurane, the abdominal cavity was opened, the liver vessels were exposed and normothermic partial hepatic ischemia was induced by the clamping of portal structures to the left and median lobes with a micro vascular clip; this yielded approximately 70% of hepatic ischemia. The abdomen was covered with saline-humidified gauze during the ischemic period. After 30 minutes of partial hepatic ischemia, the clip was removed to initiate hepatic reperfusion, the abdominal cavity was closed with a 4-0 silk suture and metal clips were applied to the skin. The temperature was maintained at 37°C during hepatic ischemia and in the post surgical period with a warming pad. Sham-operated mice underwent the same procedure without clamping of the pedicle of the liver lobes. Mice were randomly assigned to 1 of 4 group with a sample size of 4 mice per group. CGS21680 (0.5 mg/kg) was administered by intraperitoneal injection 20 min before the ischemia procedure. Mice were killed 120 min after reperfusion or employed for the procedures of liver cells isolation. For the “in vivo” analysis of liver injury, before mice sacrifice, blood was collected for serum ALT transaminase activity determination. Tissues from ischemic lobes were fixed in 4% formaldehyde and then embedded into paraffin. Sections were cut and stained with hematoxylin and eosin for histological analysis.

Liver cells isolation

Liver cells were isolated from sham operated mice or mice exposed to hepatic ischemia/reperfusion and treated or not with the A2aR agonist CGS21680 (0.5 mg/kg), after liver perfusion by collagenase digestion. After liver digestion, cells were dispersed and HP recovered by differential

centrifugation. An initial immunomagnetic separation by a mouse anti-CD45 antibody linked to immunomagnetic beads (Miltenyi biotec.) was used to collect hematopoietic cells. The negative fraction of the CD45+ cells was used to isolate LSEC by positive selection with anti-CD146 antibody linked to immunomagnetic beads. Typically, the yield of LSEC cells was $5x10^6$ per mouse liver and average of $40x10^6$ HP (15).

Cell viability estimated at the beginning of the experiments, ranged from 82% to 90%.

Isolated HP and LSEC for proteomic analysis were stored at -80°C until solubilization.

Measurement of Reactive Oxygen Species (ROS)

Cells were incubated for 10 minutes at 37°C with 5 μmol/L DCFH-DA in phosphate-buffered saline. After 2 washes with phosphate-buffered saline, cells were transferred to a fluorometer cuvette, and the fluorescence was recorded with a Hitachi F-4500 fluorescence spectrophotometer (490-nm excitation and 530-nm emission). ROS production was calculated as a percentage of the DCFH-DA fluorescence intensity versus untreated control cells.

Proteomic analysis

Samples preparation

Samples were solubilized in a solution containing 9 M urea, 4% w/v CHAPS (3-[(3-cholamidopropyl) dimethylammonio]-1-propanesulphonate), protease inhibitors and nuclease. The sample was incubated O.N. at 4°C and spun down at 13,800 g for 10 min at 4°C. The clear supernatant recovered, quantified with DC Protein assay kit and stored at -20°C until analysis.

Two-dimensional gel electrophoresis (2-DE) coomassie-stained gels

2-DE was performed using ready-made IPG strip (17-cm IPG strips, pH 3-10NL). Each sample (1 mg of total liver protein) was applied onto an IPG gel by in-gel rehydration for 20 h, adding DTT 1% w/v, final concentration and ampholine pH 3.5–10, 2% v/v, final concentration. Isoelectric focusing, strips equilibration and second dimension were performed as previously described (16). Gels were stained with colloidal Coomassie (18% v/v ethanol, 15% w/v ammonium sulfate, 2% v/v phosphoric acid, 0.2% w/v Coomassie G-250) for 48 h.

2D DIGE

Samples were labelled with CyDye DIGE Fluors following the manufacturer's instruction (GE Healthcare). Fifty micrograms of each sample was minimally labelled with 400 pmol of either

Cy 2 or Cy3 or Cy5. Cy3 and Cy5 were alternately used for samples, whereas Cy2 was used for the internal standard (a pooled standard containing total liver proteins treated or not with CGS21680). Labelling reactions were performed in the dark for 30 min on ice and then quenched with the addiction of 10mM lysine. Three 2D DIGE experiments (containing one gel each) were performed to analyse three biological replicates of control and CGS21680 or IR and CGS21680+IR samples. 2-DE was performed as described above.

Image analysis

Gel images were acquired with ChemiDoc Imaging System (Bio-Rad).

Image analysis was performed using PD-Quest software (version 7.2, Bio-Rad) according to the manufacturer's instructions. Normalization of each individual spot was performed according to the total quantity of the valid spots in each gel, after subtraction of the background values. The spot volume was used as the analysis parameter to quantify protein expression.

Protein identification by mass spectrometry and database search

Coomassie G-stained spots were excised from 2-DE preparative gels; destaining and in-gel enzymatic digestion performed as previously described (16). All digests were analyzed by MALDI-TOF (TofSpec SE, MicroMass) equipped with a delayed extraction unit. Peptides solution was prepared with equal volumes of saturated a-cyano-4-hydroxycinnamic acid solution in 40% v/v acetonitrile-0.1% v/v trifluoroacetic acid. The MALDI-TOF was calibrated with a mix of PEG (PEG 1000, 2000 and 3000 with the ratio 1:2:2) and mass spectra were acquired in the positive-ion mode. Peak lists were generated with ProteinLynx Data Preparation (ProteinLynx Global Server 2.2.5) using the following parameters: external calibration with lock mass using mass 2465.1989 Da of ACTH, background subtract type adaptive combining all scans, performing deisotoping with a threshold of 1%. The 25 most intense masses were used for database searches against the SWISSPROT database using the free search program MASCOT (http://www.matrixscience.com). The following parameters were used in the searches: taxa Mus musculus, trypsin digest, one missed cleavage by trypsin, carbamidomethylation of cysteine as fixed modification, methionine oxidation as variable modifications and maximum error allowed 100 ppm. Were taken on to consideration only protein with a Mascot score≥56.

Western blotting

Lysates containing equal amounts of proteins (30 μg), containing Laemmli buffer, were subjected to SDS/PAGE (12% gel). The separated proteins were transferred to a nitrocellulose membrane. The blot was blocked using 5% w⁄v dried no fatty milk in PBS containing 0.1% Tween-20, and probed using rabbit antibody against arginase 1 (diluted 1:1000), mouse antibody against α-enolase (diluted 1:5000), rabbit antibody against 3-ketoacyl-CoA thiolase (diluted 1:3000) overnight at 4°C. After washing using PBS containing 0.1% Tween-20 for 30 min, the blot was incubated for 1 h with horseradish-peroxidase labeled antibodies against rabbit or mouse IgG (diluted 1:10000), and immunoreactivity was detected using an enhanced chemiluminescence kit.

Real-time quantitative RT-PCR

Total RNA was isolated from frozen isolated HP and LSEC taken from sham liver or liver exposed to ischemia-reperfusion from mice treated or not with CGS21680, using the ChargeSwitch® Total RNA Cell Kit (Applied Biosystems Italia, Monza, Italy) following manufacturer's instructions. RNA was reverse transcribed for first-strand complementary DNA (cDNA) synthesis using High Capacity cDNA Reverse Transcription Kit (Applied Biosystems Italia, Monza, Italy) according to the manufacturer's recommendations. Quantitative real-time polymerase chain reaction (RT-PCR) was performed in the CFX96 Touch™ Real-Time PCR Detection System-Bio-Rad (Bio-Rad Laboratories S.r.l, Milan, Italy) using TaqMan Gene Expression Master Mix and Taqman Gene Expression probes for mouse 3-ketoacyl-CoA thiolase (THIM), arginase1 (ARGI1), α-enolase (ENOA), and β-actin or 18S as control genes (Applied Biosystems Italia, Monza, Italy). All samples were ran in duplicate, and the relative gene expression calculated as $2^{-\Delta Ct}$ is expressed as fold increase over control samples. Values were normalized to those of β-actin for ENOA or to those of 18S for THIM and ARGI1 and expressed by using the comparative $2^{-\Delta Ct}$ method.

Enzymatic assays

Glycid metabolism

Cells were rinsed with PBS, sonicated with 10 bursts of 1 s, centrifuged at 13,000 x g for 5 min, re-suspended in 100 mmol/L Tris (pH 7.4). A 50 µL aliquot was used for the protein quantification with the BCA Kit (Sigma Chemical Co., St. Louis, MO). 50 µg of whole cell lysates were used in each assay.

Aldolase B activity was measured as described in (17), with minor modifications: samples were incubated at 37°C, in the presence of 100 mmol/L K_2HPO_4 (pH 7.2), 1 mmol/L fructose 1,6-biphosphate, 10 mmol/L EDTA, 2 mg/mL α-glycerophosphate dehydrogenase, 2 mg/mL triose phosphate

isomerase, 100 µg/mL bovine serum albumin, 0.15 mmol/L NADH, in a final volume of 300 µL. The rate of NADH oxidation was followed for 5 min, monitoring the absorbance at 340 nm with a Packard microplate reader EL340 (Bio-Tek Instruments, Winooski, VT). Results were expressed as nmol NADH produced/min/mg cell proteins. Enolase A activity was measured accordingly to (18). Results were expressed as nmol NAD^+/min/mg cell proteins.

The activity of pyruvate kinase was detected with the Enzymatic Assay of Pyruvate Kinase kit, following the manufacturer's instruction. Results were expressed as nmol NAD^+/min/mg cell proteins.

Lipid metabolism

Fatty acids β-oxidation was measured as previously reported (19), with minor modifications. Cells were washed twice with PBS, detached with trypsin/EDTA (0.05/0.02% v/v) and centrifuged at 13,000 x g for 5 min. A 50 µL aliquot was collected, sonicated and used for the intracellular protein quantification. The remaining sample was re-suspendend in culture medium containing 0.24 mmol/L fatty acid-free bovine serum albumin, 0.5 mmol/L L-carnitine, 20 mmol/L Hepes, 2 µCi [1-^{14}C]palmitic acid (3.3 mCi/mmol) and transferred into test tubes tightly sealed with rubber caps. After 2 h incubation at 37°C, 0.3 mL of a 1:1 v/v phenylethylamine/methanol solution was added into each sample by a syringe, followed by 0.3 mL of 0.8 N $HClO_4$. Samples were incubated for 1 h further at room temperature, then centrifuged at 13,000 x g for 10 min. Both supernatants, containing $^{14}CO_2$, and precipitates, containing ^{14}C-acid soluble metabolites (ASM), were collected. The radioactivity of each sample was counted by liquid scintillation. Results were expressed as pmol of [$^{14}CO_2$] or ^{14}C-ASM/h/mg cell proteins.

Aminoacid metabolism

The activity of carbamoyl phosphate synthetase I was measured on mitochondrial extracts, isolated as reported previously (20). Samples were sonicated and a 50 µL aliquot was used for protein quantification . 25 µg of mitochondrial proteins were incubated in 0.5 mL of the assay buffer (87 mmol/L Tris/HCl, 87 mmol/L KCl, 25 mmol/l $MgCl_2$, 10 mmol/L ATP, 20 mmol/L NH_4Cl, 0.8 mmol/L dithiothreitol, 6.5% v/v dimethyl sulfoxide, 2.2% v/v glycerol) with 4 µCi [^{14}C]-$NaHCO_3$ (54 mCi/mmol) for 30 minutes at 37°C. The reaction was stopped by adding 0.2 mL of 80% w/v trichloroacetic acid. To remove the unincorporated $^{14}CO_2$, the tubes were heated at 85°C for 3 h; the remaining samples, containing [^{14}C]-carbamoyl phosphate, were analyzed by liquid scintillation counting. Results were expressed as pmol carbamoyl phosphate/min/mg cell proteins.

Arginase activity was measured on 50 µg of whole cell lysates by a spectrophotometric method (21). Results were expressed as µmol urea/mg cell proteins.

Mitochondrial metabolism

Mitochondria were isolated as reported above.

To measure the isocitrate dehydrogenase activity, 25 µg mitochondrial proteins were re-suspended in 0.3 mL of Tris-acetate (pH 7.4), containing 5 mmol/L DL-isocitrate trisodium salt and 5 mmol/L $MgCl_2$. The reaction was started by adding 0.5 mmol/L NAD^+ and the absorbance at 340 nm was followed for 5 minute. Results were expressed as nmol NADH/mg mitochondrial proteins.

The rate of cytochrome c reduction was taken as an index of the activity of the electron flux from complex I to complex III, and was measured according to (22) with minor modifications. 50 µg of non-sonicated mitochondrial samples, re-suspended in 0.59 mL buffer A (5 mmol/L KH_2PO_4, 5 mmol/L $MgCl_2$, 5% w/v bovine serum albumin), were transferred into a quartz spectrophotometer cuvette. Then 0.38 mL buffer B (25% w/v saponin, 50 mmol/L KH_2PO_4, 5 mmol/L $MgCl_2$, 5% w/v bovin serum albumin, 0.12 mmol/L cytochrome c-oxidized form, 0.2 mmol/L NaN_3) were

added for 5 min at room temperature. The reaction was started with 0.15 mmol/L NADH and was followed for 5 min, reading the absorbance at 550 nm by a Lambda 3 spectrophotometer (PerkinElmer).

The ATP level in mitochondria extracts was measured with the ATP Bioluminescent Assay Kit, using a Synergy HT Multi-Mode Microplate Reader (Bio-Tek Instruments). ATP was quantified as arbitrary light units and converted into nmol ATP/mitochondrial proteins, according to the calibration curve previously set.

Supplementary Tables

PROTEINS ABBREVIATIONS

ABHEB (Abhydrolase domain-containing protein 14B); **ALDH2** (Aldehyde dehydrogenase, mitochondrial); **AL4A1** (Delta-1-pyrroline-5-carboxylate dehydrogenase, mitochondrial); **ALDOB** (Fructose-bisphosphate aldolase B); **ATPA** (ATP syntase A), **ATPB** (ATP syntase B); **ATP5H** (ATP synthase subunit d, mitochondrial); **ARGI1** (Arginase-1); **ASXL3** (Putative Polycomb group protein ASXL3); **CAH3** (Carbonic anhydrase 3); **CALM** (Calmodulin); **CATA** (Catalase); **CATB** (Cathepsin B); **CH60** (60 kDa heat shock protein, mitochondrial); **CHD1** (Chromodomain-helicase-DNA-binding protein 1); **CJ088** (Uncharacterized protein C10orf88 homolog); **CK054** (Ester hydrolase C11orf54 homolog); **CLC4F** (C-type lectin domain family 4 member F); **CPSM** (Carbamoyl-phosphate synthase [ammonia], mitochondrial); **DHSO** (Sorbitol dehydrogenase); **DNM3A** (DNA (cytosine-5)-methyltransferase 3); **ECH1** (Delta(3,5)-Delta(2,4)-dienoyl-CoA isomerase, mitochondrial); **EF1B** (Elongation factor 1-beta); **EF2** (Elongation factor 2); **ENOA** (Alpha-enolase); **ETFA** (Electron transfer flavoprotein subunit alpha, mitochondrial); **FAAA** (Fumarylacetoacetase); **FABP5** (Fatty acid-binding protein, epidermal); **FABPI** (Fatty acid-binding protein, intestinal); **FABPL** (Fatty acid-binding protein, liver); **FKB1B** (Peptidyl-prolyl cis-trans isomerase FKBP1B); **GLYC** (Serine hydroxymethyltransferase, cytosolic); **GRP75** (Stress-70 protein, mitochondrial); **GSTM1** (Glutathione S-transferase Mu 1); **GSTP1** (Glutathione S-transferase P 1); **GSTP2** (Glutathione S-transferase P 2); **3HAO** (3-hydroxyanthranilate 3,4-dioxygenase); **HINT1** (Histidine triad nucleotide-binding protein 1); **IDHC** (Isocitrate dehydrogenase [NADP] cytoplasmic); **IPYR** (Inorganic pyrophosphatase); **K2C8** (Keratin, type II cytoskeletal 8); **KPYR** (Pyruvate kinase isozymes R); **MCM2** (DNA replication licensing factor MCM2); **MIC1** (Uncharacterized protein C18orf8 homolog); **MUP8** (Major urinary proteins 8 (Fragment)); **NDKB** (Nucleoside diphosphate kinase B); **ODBA** (2-oxoisovalerate dehydrogenase subunit alpha, mitochondrial); **OTC** (Ornithine carbamoyltransferase, mitochondrial); **PDIA1** (Protein disulfide-isomerase); **PDIA3** (Protein disulfide-isomerase A3); **PEBP1** (Phosphatidylethanolamine-binding protein 1); **PGK1** (Phosphoglycerate kinase 1); **PPIA** (Peptidyl-prolyl cis-trans isomerase A); **PRDX6** (Peroxiredoxin-6); **PROSC** (Proline synthase co-transcribed bacterial homolog protein); **RGN** (Regucalcin); **ROA2** (Heterogeneous nuclear ribonucleoproteins A2); **S2542** (Solute carrier family 25 member 42); **SBP2** (Selenium-binding protein 2); **SNX5** (Sorting nexin-5); **THIM** (3-ketoacyl-CoA thiolase); **TPIS** (Triosephosphate isomerase); **VDAC1** (Voltage-dependent anion-selective channel protein 1)

Table 1. IR modulated spots Spot number (SSP), accession number on SwissProt database (AC), name, densitometric ratio between IR and control sample, p value, biological function, number of matched mass values (match. pept.) on number of total mass values searched (25), coverage percentage and Mascot score are indicated.

	SSP		AC	name	IR/control	p value	function	Match. pept./ 25	coverage %	Mascot score
HP	1506	EF1B	O70251	Elongation factor 1-beta	0,11	0,002	protein biosynthesis	5	24	56
	2503	Mixture			0,34	0,038				108
		RGN	Q64374	Regucalcin			calcium binding protein; vitamine C biosynthesis	8	31	88
		KPYR	P53657	Pyruvate kinase isozymes R/L			metabolism, glycolysis	7	18	60
	2602	ATPB	Q3U774	ATP synthase subunit beta, mitochondrial	0,25	0,009	metabolism, oxidative phosphorylation	15	44	192
	4303	FABPI	P55050	Fatty acid-binding protein, intestinal	0,32	0,013	metabolism, lipid binding protein	8	54	106
	4703	ENOA	P17182	Alpha-enolase	0,21	0,032	metabolism, glycolysis	9	36	116
	6402	ATPA	Q03265	ATP synthase subunit alpha, mitochondrial	0,39	0,015	metabolism, oxidative phosphorylation	8	21	61
LSEC	701	PDIA1	P09103	Protein disulfide-isomerase	0,18	0,054	stress protein	12	28	126
	1604	ATPB	Q3U774	ATP synthase subunit beta, mitochondrial	0,14	0,029	metabolism, oxidative phosphorylation	16	45	222
	3505	CLC4F	P70194	C-type lectin domain family 4 member F	0,20	0,039	metabolism, receptor with an affinity for galactose and fucose	7	15	56
	5512	CATA	P24270	Catalase	0,05	0,040	stress protein	9	24	93
	5515	ODBA	P50136	2-oxoisovalerate dehydrogenase subunit	0,26	0,015	metabolism,	13	38	138

				alpha, mitochondrial			conversion of alpha-keto acids to acyl-CoA and CO2			
	5908	CJ088	Q9D2Q3	Uncharacterized protein C10orf88 homolog	0,12	0,016	unknown	6	18	57
	7406	NDKB	Q01768	Nucleoside diphosphate kinase B	0,26	0,035	metabolism, synthesis of nucleoside triphosphates other than ATP	11	69	132
	8409	ROA2	O88569	Heterogeneous nuclear ribonucleoproteins A2/B1	0,25	0,052	pre-mRNA processing	6	20	57

Table 2. CGS modulated spots Spot number (SSP), accession number on SwissProt database (AC), name, densitometric ratio between CGS and control sample, p value, biological function number of matched mass values (match. pept.) on number of total mass values searched (25), coverage percentage and Mascot score are indicated.

	SSP		AC	name	CGS/control	p value	function	match. pept./ 25	coverage %	Mascot score
HP	1604	IPYR	Q9D819	Inorganic pyrophosphatase	3,22	0,018	pyrophosphatase	10	42	122
	4901	GLYC	P50431	Serine hydroxymethyltransferase, cytosolic	0,48	0,025	metabolism, aminoacids	9	25	87
	5609	IDHC	O88844	Isocitrate dehydrogenase [NADP] cytoplasmic	4,74	0,009	metabolism, Krebs cycle	7	25	64
	9949	FABPL	P12710	Fatty acid-binding protein, liver	5,58	0,031	metabolism, lipids binding protein	6	61	82
LSEC	3410	Mixture			4,41	0,001				75
		OTC	P11725	Ornithine carbamoyltransferase, mitochondrial			metabolism, urea cycle	6	22	59
		PGK1	P09411	Phosphoglycerate kinase 1			metabolism, glycolisis	6	26	57
	5602	ENOA	P17182	Alpha-enolase	1,67	0,051	metabolism, glycolisis	13	44	154
	8604	THIM	Q8BWT1	3-ketoacyl-CoA thiolase, mitochondrial	2,84	0,052	metabolism, fatty acids beta oxidation	13	51	166

Table 3. CGS+IR modulated spots Spot number (SSP), accession number on SwissProt database (AC), name, densitometric ratio between CGS+IR and control, CGS or IR sample, p value, biological function, number of matched mass values (match. pept.) on number of total mass values searched (25), coverage percentage and Mascot score are indicated.

	SSP		AC	name	CGS+IR/ control	p value	function	match. pept./ 25	coverage %	Mascot score
HP	804	GRP75	P38647	Stress-70 protein, mitochondrial	0,47	0,042	stress protein	7	14	61
	2202	FABPI	P55050	Fatty acid-binding protein, intestinal	5,51	0,039	metabolism, lipids binding protein	8	54	106
	2203	ABHEB	Q8VCR7	Abhydrolase domain-containing protein 14B	4,19	0,051	hydrolase activity towards p-nitrophenyl butyrate	5	37	64
	4202	GSTP1	P19157	Glutathione S-transferase P 1	0,46	0,007	stress protein	7	40	84
	4803	ARGI1	Q61176	Arginase-1	2,99	0,029	metabolism, urea cycle	10	40	105
	8201	MCM2	P97310	DNA replication licensing factor MCM2	13,09	0,020	DNA replication	10	12	62
	9105	FABPL	P12710	Fatty acid-binding protein, liver	0,26	0,030	metabolism, lipids binding protein	7	60	78
LSEC	3301	ATP5H	Q9DCX2	ATP synthase subunit d, mitochondrial	5,79	0,029	metabolism, oxidative phosphorylation	5	39	58
	4401	OTC	P11725	Ornithine carbamoyltransferase, mitochondrial	22,01	0,012	metabolism, urea cycle	6	19	57
	4605	Mixture			6,20	0,014				75
		OTC	P11725	Ornithine carbamoyltransferase, mitochondrial			metabolism, urea cycle	6	22	59
		PGK1	P09411	Phosphoglycerate kinase 1			metabolism, glycolisis	6	26	57
	4702	CATA	P24270	Catalase	15,27	0,019	stress protein	9	24	93
	6210	FABPL	P12710	Fatty acid-binding protein, liver	7,38	0,049	metabolism, lipids binding protein	7	51	60
	6212	ASXL3	Q8C4A5	Putative Polycomb group protein ASXL3	110,23	0,002	transcriptional control	12	8	56

	7702	THIM	Q8BWT1	3-ketoacyl-CoA thiolase, mitochondrial	3,15	0,044	metabolism, fatty acids beta oxidation	8	28	82
	SSP		**AC**	**name**	**CGS+IR/ CGS**	**p value**	**function**	**match. pept./ 25**	**coverage %**	**Mascot score**
HP	1502	K2C8	P11679	Keratin, type II cytoskeletal 8	0,27	0,035	structural	11	24	106
	2504	Mixture			3,70	0,042				108
		RGN	Q64374	Regucalcin			calcium binding protein; vitamine C biosynthesis	8	31	88
		KPYR	P53657	Pyruvate kinase isozymes R/L			metabolism, glycolysis	7	18	60
	3502	IPYR	Q9D819	Inorganic pyrophosphatase	0,35	0,027	pyrophosphatase	10	42	122
	3601	ENOA	P17182	Alpha-enolase	2,47	0,033	metabolism, glycolysis	9	27	92
	3702	SBP2	Q63836	Selenium-binding protein 2	3,69	0,018	stress protein	10	33	121
	3705	SBP2	Q63836	Selenium-binding protein 2	2,77	0,029	stress protein	11	29	134
	3708	GRP75	P38647	Stress-70 protein, mitochondrial	5,09	0,010	stress, folding of proteins	9	16	82
	4401	3HAO	Q78JT3	3-hydroxyanthranilate 3,4-dioxygenase	2,98	0,045	cofactor biosynthesis	6	31	61
	4501	ARGI1	Q61176	Arginase-1	3,59	0,004	metabolism, urea cycle	9	40	103
	4706	ENOA	P17182	Alpha-enolase	0,25	0,021	metabolism, glycolysis	9	36	116
	4707	ALDH2	P47738	Aldehyde dehydrogenase, mitochondrial	4,52	0,011	stress protein	14	33	181
	5203	PPIA	P17742	Peptidyl-prolyl cis-trans isomerase A	3,25	0,027	folding of proteins	5	24	74
	5302	GSTM1	P10649	Glutathione S-transferase Mu 1	3,63	0,043	stress, folding of proteins	7	39	75
	5502	ARGI1	Q61176	Arginase-1	6,34	0,055	metabolism, urea cycle	10	36	112
	5504	DHSO	Q64442	Sorbitol dehydrogenase	3,08	0,026	metabolism, sorbitol to fructose conversion	7	32	71

	5505	Mixture			4,89	0,004				106
		DHSO	Q64442	Sorbitol dehydrogenase			metabolism, sorbitol to fructose conversion	8	36	86
		ARGI1	Q61176	Arginase-1			metabolism, urea cycle	6	25	58
	5506	ARGI1	Q61176	Arginase-1	5,21	0,015	metabolism, urea cycle	10	40	105
	5508	ALDOB	Q91Y97	Fructose-bisphosphate aldolase B	3,59	0,026	metabolism, glycolysis	6	20	56
	5603	FAAA	P35505	Fumarylacetoacetase	3,81	0,051	metabolism, aa degradation	10	39	108
	5701	ENOA	P17182	Alpha-enolase	2,37	0,050	metabolism, glycolysis	13	44	154
	6203	MIC1	Q8VC42	Uncharacterized protein C18orf8 homolog	2,52	0,021	unknown	7	20	70
	6302	ATPA	Q03265	ATP synthase subunit alpha, mitochondrial	1,85	0,029	metabolism, oxidative phosphorylation	8	21	61
	6402	ETFA	Q99LC5	Electron transfer flavoprotein subunit alpha, mitochondrial	4,14	0,038	metabolism, oxidative phosphorylation	8	39	92
	7401	CAH3	P16015	Carbonic anhydrase 3	2,58	0,036	reversible hydration of carbon dioxide	12	51	168
	9402	VDAC1	Q60932	Voltage-dependent anion-selective channel protein 1	2,41	0,042	cell volume regulation and apoptosis	7	44	89
	9601	THIM	Q8BWT1	3-ketoacyl-CoA thiolase, mitochondrial	3,37	0,020	metabolism, fatty acids beta oxidation	11	39	136
LSEC	2105	DNM3A	O88508	DNA (cytosine-5)-methyltransferase 3A	27,48	0,043	DNA methylation	9	11	66
	2201	PROSC	Q9Z2Y8	Proline synthase co-transcribed bacterial homolog protein	8,96	0,013	metabolism, aminoacids	5	20	57
	2203	MUP8	P04938	Major urinary proteins 11 and 8 (Fragment)	2,71	0,053	pheromones binding	10	78	130
	2308	PEBP1	P70296	Phosphatidylethanol	0,24	0,053	ATP, opioids and	8	60	124

				amine-binding protein 1			phosphatidylethanolamine binding			
	3201	ATP5H	Q9DCX2	ATP synthase subunit d, mitochondrial	0,48	0,036	metabolism, oxidative phosphorylation	5	39	58
	3304	PRDX6	O08709	Peroxiredoxin-6	92,13	0,002	stress protein	8	32	98
	3601	ATPB	Q3U774	ATP synthase subunit beta, mitochondrial	9,79	0,003	metabolism, oxidative phosphorylation	15	44	184
	3701	CH60	P63038	60 kDa heat shock protein, mitochondrial	0,32	0,021	stress protein	10	32	98
	5304	PRDX6	O08709	Peroxiredoxin-6	11,16	0,010	stress protein	8	51	111
	5401	PDIA3	P27773	Protein disulfide-isomerase A3	4,37	0,021	stress protein	12	25	129
	5501	Mixture			5,04	0,010				213
		3HAO	Q78JT3	3-hydroxyanthranilate 3,4-dioxygenase OS=Mus musculus			catalyzes the oxidative ring opening of 3-hydroxyanthranilate to 2-amino-3-carboxymuconate semialdehyde, which spontaneously cyclizes to quinolinate	11	52	131
		ECH1	O35459	Delta(3,5)-Delta(2,4)-dienoyl-CoA isomerase, mitochondrial			metabolism, fatty acids beta oxidation	11	48	114
	6302	EF2	P58252	Elongation factor 2	18,04	0,006	protein synthesis	14	18	115
	7302	CPSM	Q8C196	Carbamoyl-phosphate synthase [ammonia], mitochondrial	15,04	0,001	metabolism, urea cycle	11	9	64
	7606	FAAA	P35505	Fumarylacetoacetase	0,10	0,012	metabolism, aminoacids degradation	6	24	69
	9105	GSTP2	P46425	Glutathione S-transferase P 2	16,76	0,052	stress protein	5	39	60
	9701	AL4A1	Q8CHT0	Delta-1-pyrroline-5-	8,06	0,035	metabolism,	7	23	78

				carboxylate dehydrogenase, mitochondrial			aminoacids degradation			
	9702	Mixture			0,33	0,056				84
		CHD1	P40201	Chromodomain-helicase-DNA-binding protein 1			DNA replication	12	9	70
		ATPA	Q03265	ATP synthase subunit alpha, mitochondrial			metabolism, oxidative phosphorylation	8	18	61
	SSP		**AC**	**name**	**CGS+IR/ IR**	**p value**	**function**	**match. pept./ 25**	**coverage %**	**Mascot score**
HP	202	CALM	Q498A3	Calmodulin	2,51	0,020	control of a large number of enzymes, ion channels and other proteins by Ca^{2+}	5	50	57
	3701	SBP2	Q63836	Selenium-binding protein 2	2,82	0,017	stress protein	10	30	114
	3705	SBP2	Q63836	Selenium-binding protein 2	3,55	0,040	stress protein	11	29	134
	4501	ARGI1	Q61176	Arginase-1	2,21	0,022	metabolism, urea cycle	9	40	103
	5504	DHSO	Q64442	Sorbitol dehydrogenase	2,44	0,044	metabolism, sorbitol to fructose conversion	7	32	71
	5505	Mixture			2,36	0,021				106
		DHSO	Q64442	Sorbitol dehydrogenase			metabolism, sorbitol to fructose conversion	8	36	86
		ARGI1	Q61176	Arginase-1			metabolism, urea cycle	6	25	58
	5506	ARGI1	Q61176	Arginase-1	2,62	0,036	metabolism, urea cycle	10	40	105
	5602	GLYC	P50431	Serine hydroxymethyltransferase, cytosolic	2,35	0,013	metabolism, aminoacids	9	25	87
	5603	FAAA	P35505	Fumarylacetoacetase	2,99	0,051	metabolism, aminoacids degradation	10	39	108
	5701	ENOA	P17182	Alpha-enolase	2,95	0,037	metabolism, glycolysis	13	44	154
	6401	CPSM	Q8C196	Carbamoyl-phosphate synthase	3,04	0,002	metabolism, urea cycle	10	8	65

				[ammonia], mitochondrial						
	7301	Mixture			2,94	0,045				98
		TPIS	P17751	Triosephosphate isomerase			metabolism, glycolysis	7	28	77
		S2542	Q8R0Y8	Solute carrier family 25 member 42			metabolism, transport of coenzyme A (CoA) in mitochondria	7	23	56
	7604	THIM	Q8BWT1	3-ketoacyl-CoA thiolase, mitochondrial	3,46	0,041	metabolism, fatty acids beta oxidation	8	28	82
	8302	GSTP1	P19157	Glutathione S-transferase P 1	2,88	0,031	stress protein	5	37	61
	8602	THIM	Q8BWT1	3-ketoacyl-CoA thiolase, mitochondrial	3,84	0,033	metabolism, fatty acids beta oxidation	13	51	166
	8605	THIM	Q8BWT1	3-ketoacyl-CoA thiolase, mitochondrial	5,35	0,045	metabolism, fatty acids beta oxidation	14	39	173
	8607	THIM	Q8BWT1	3-ketoacyl-CoA thiolase, mitochondrial	5,34	0,030	metabolism, fatty acids beta oxidation	8	28	82
	9502	FKB1B	Q9Z2I2	Peptidyl-prolyl cis-trans isomerase FKBP1B	3,30	0,004	folding of proteins	5	38	66
	9601	THIM	Q8BWT1	3-ketoacyl-CoA thiolase, mitochondrial	2,51	0,034	metabolism, fatty acids beta oxidation	11	34	124
LSEC	1303	SNX5	Q9D8U8	Sorting nexin-5	27,99	0,028	intracellular trafficking	6	24	57
	1405	CATB	P10605	Cathepsin B	10,43	0,004	intracellular degradation and turnover of proteins	6	23	66
	2909	GRP75	P38647	Stress-70 protein, mitochondrial	6,15	0,040	stress protein	9	17	72
	2912	GRP75	P38647	Stress-70 protein, mitochondrial	11,47	0,017	stress protein	8	15	57
	3101	FABP5	Q05816	Fatty acid-binding protein, epidermal	4,13	0,002	metabolism, lipids binding protein	5	31	59
	3303	PRDX6	O08709	Peroxiredoxin-6	8,23	0,052	stress protein	8	51	111

	3404	CK054	Q91V76	Ester hydrolase C11orf54 homolog	7,03	0,003	ester hydrolase activity on the substrate p-nitrophenyl acetate	8	30	104
	4103	HINT1	P70349	Histidine triad nucleotide-binding protein 1	3,70	0,006	Hydrolyzes purine nucleotide phosphoramidates with a single phosphate group	7	71	97
	5301	ETFA	Q99LC5	Electron transfer flavoprotein subunit alpha, mitochondrial	3,69	0,035	metabolism, oxidative phosphorylation	6	31	63
	5502	ARGI1	Q61176	Arginase-1	5,69	0,020	metabolism, urea cycle	11	49	136
	7104	PPIA	P17742	Peptidyl-prolyl cis-trans isomerase A	3,52	0,052	folding of proteins	5	34	59

Supplementary Figure 1

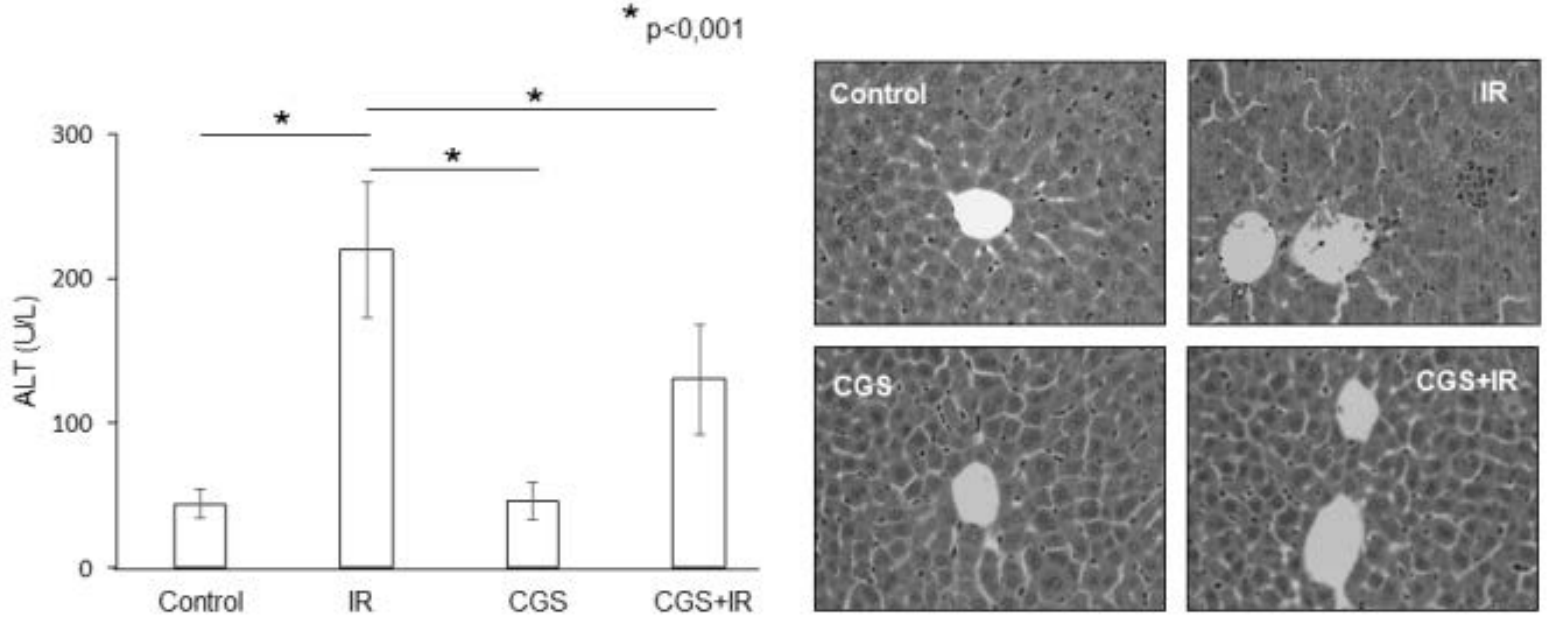

Supplementary Figure 1 The administration of CGS21680 ameliorates liver IR injury.

Liver IR damage was induced by 30 minutes of warm ischemia followed by 120 minutes of reperfusion. CGS21680 (0.5 mg/kg) was injected intraperitoneally 20 min before liver ischemia. Sham-operated mice were used as controls. Hepatic injury was evaluated by the measurement of serum ALT release or at histology . Results are mean ± SD of 6 experiments. * $p < 0.05$.

Supplementary Figure 2

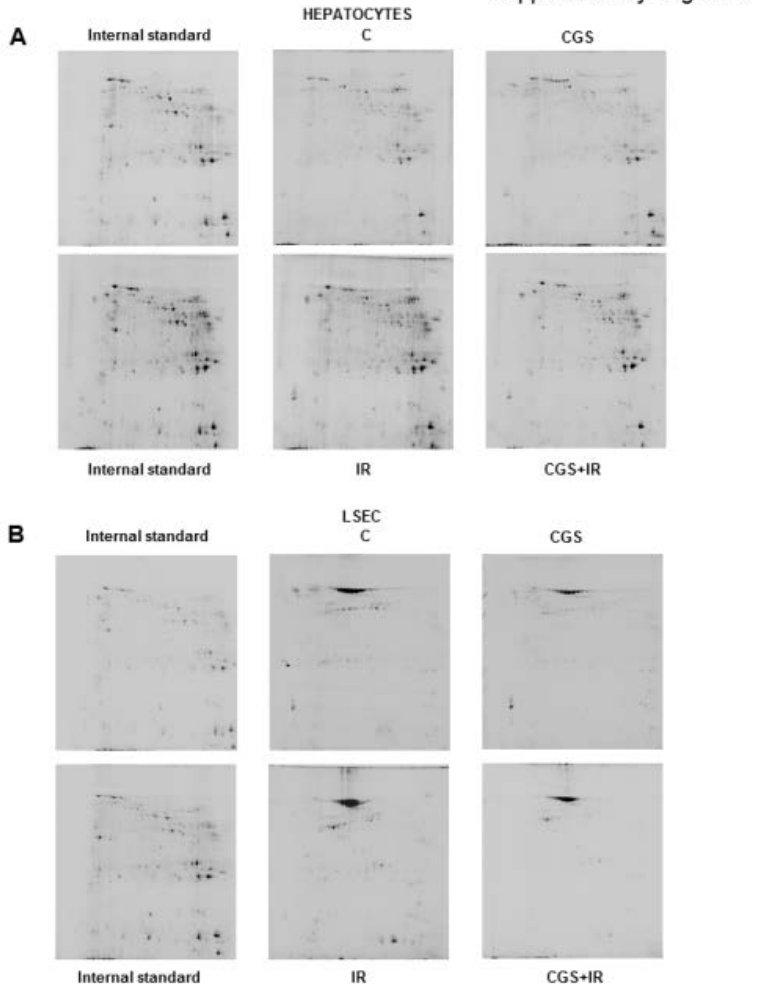

Supplementary Figure 2 2D-DIGE Representative images (of three independent experiments) of 2DE DIGE gels. Hepatocytes (A) and LSEC (B) proteins expression were studied in control conditions and upon A2aR stimulation with the A2aR agonist CGS21680 (CGS) or IR in presence (CGS+IR) and in absence (IR) of CGS21680. Internal standard gels are also reported.

Supplementary Figure 3

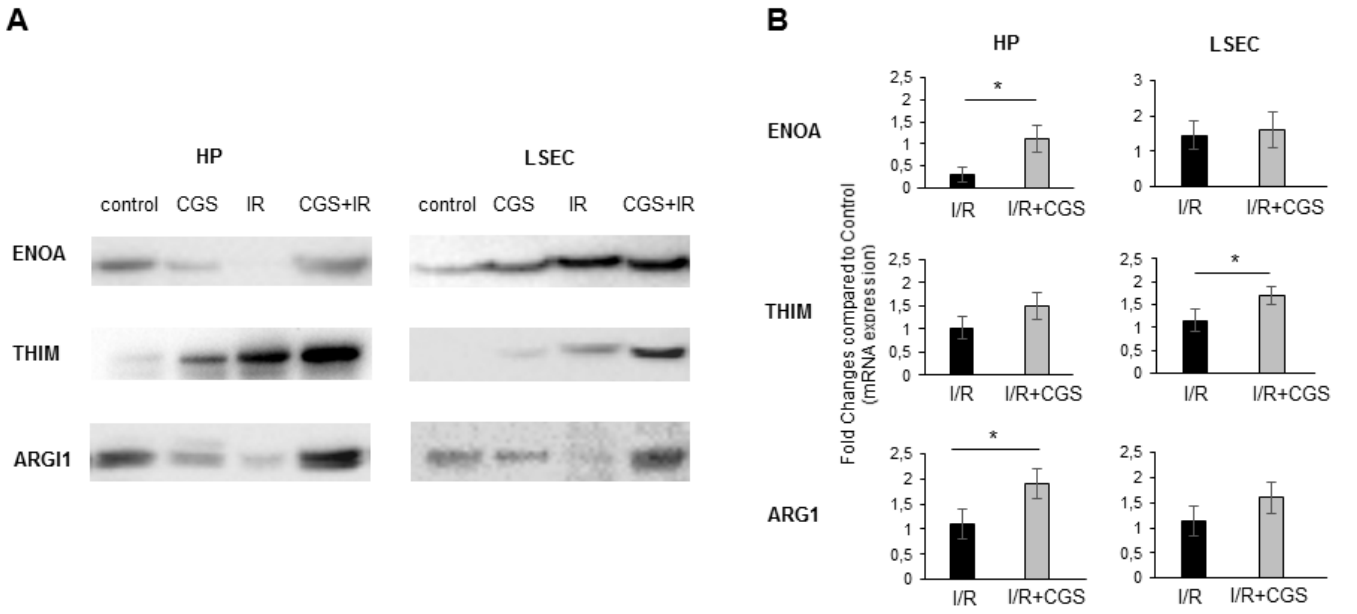

Supplementary Figure 3 Western blot and RT-PCR analysis of ENOA, THIM and ARGI1 (A) Representative western blot (of three independent experiments) with anti-ENOA, anti-THIM and anti-ARGI1 antibodies. HP and LSEC proteins expression were analyzed in control conditions (control) or upon A2aR stimulation with the A2aR agonist CGS21680 (CGS) or IR in presence (CGS+IR) or in absence (IR) of CGS21680. (B) Total RNA was isolated from HP and LSEC from sham mice (control) or mice exposed to IR and pretreated or not with CGS21680 (CGS) and ENOA, THIM and ARG-1 were determined by quantitative RT- PCR. Results are mean ± SD of 3 independent experiments. * $p < 0.05$.